Journal of Hazardous Materials 203–204 (2012) 251–256

Contents lists available at SciVerse ScienceDirect

Journal of Hazardous Materials

journal homepage: www.elsevier.com/locate/jhazmat

Removal of benzene and methyl ethyl ketone vapor: Comparison of hypercrosslinked polymeric adsorbent with activated carbon

Chao Long*, Ying Li, Weihua Yu, Aimin Li

State Key Laboratory of Pollution Control and Resource Reuse, School of the Environment, Nanjing University, 163 Xianlin Road, Nanjing 210046, China

ARTICLE INFO

Article history:
Received 13 July 2011
Received in revised form 4 November 2011
Accepted 5 December 2011
Available online 13 December 2011

Keywords:
Hypercrosslinked polymeric resin
Activated carbon
VOCs
Adsorption
Isosteric heat

ABSTRACT

A novel hypercrosslinked polymeric adsorbent (HY-1) with high surface area and specific bimodal pore size distribution in the regions of micropore (0.5–2.0 nm) and meso-macropore (30–70 nm) was prepared. Adsorption properties of benzene and methyl ethyl ketone (MEK) vapors onto HY-1 were investigated and compared with a commercial microporous activated carbon (m-GAC). The equilibrium adsorption data showed that the adsorption capacities of benzene and MEK on HY-1 were larger than those of m-GAC at the higher relative pressure. The Dubinin–Radushkevich (D–R) equation was found to fit the experimental data well. The isosteric enthalpy of adsorption for benzene and MEK were calculated. The m-GAC exhibited much higher values of ΔH_{st} for the VOCs than HY-1 at the whole loading studied, which can lead to significant temperature rises during the adsorption step. The results of dynamic experiments revealed that HY-1 had a good dynamic adsorption capacity with a longer breakthrough time and shorter length of mass transfer zone due to its specific bimodal property. Therefore, HY-1 will be a particularly efficient and competitive adsorbent for VOCs recovery, especially at medium-high concentrations.

1. Introduction

Volatile organic compounds (VOCs) have been widely used as dissolving and cleaning agents in many industrial processes. The emission of solvent vapors from these industrial processes has caused not only severe air pollution but also great loss of valuable chemicals. Therefore, it has already received great attention to develop efficient and economical control strategies for recovering VOCs vapor from industries [1]. Activated carbon is applied extensively for the removal of VOCs from gas streams with subsequent solvent recovery or incineration [2–6]. However, it has been recognized that activated carbon adsorption always encounters some problems such as combustion, pore blocking, inefficiently desorption of high-boiling solvents, and hygroscopicity [7–9]. Hence, much effort has been focused at finding alternative adsorbents to separate and recover VOCs from polluted air streams.

In the past few decades, the permanently porous polymeric adsorbents have become effective for the removal of organic pollutants from aqueous streams due to its controllable pore structure, stable physical, chemical properties and regenerability on site as well as vast surface area comparable to activatedcarbon [10]. Of the porous polymers, hypercrosslinked polymeric adsorbent, which is produced by further crosslinking polymers in a good solvent, represents a class of predominantly microporous organic materials with large specific surface area and high micropore volume [11,12]. Now hypercrosslinked polymeric resin produced by many manufactures worldwide is finding increased application as sorbents for separation or analytical purposes and water pollution control [13–17]. However, to the best of our knowledge, there are only limited studies done on hypercrosslinked polymeric resin as adsorbents for removing the VOCs from gas steam currently [18–24].

In the present study we synthesized a novel hypercrosslinked polymeric adsorbent (HY-1) with high surface area and specific bimodal pore size distribution in the regions of micropore (0.5–2.0 nm) and meso-macropore (30–70 nm). The adsorption characteristics of HY-1 was evaluated and compared with a commercial microporous activated carbon (m-GAC). Thus, adsorption equilibrium of benzene and MEK vapors onto HY-1 and m-GAC at 303, 318, and 333 K were investigated. For better understanding of adsorption properties, the isosteric enthalpies of adsorption were calculated, which is very important to evaluate the molecular scale interactions between adsorbate and adsorbent and to investigate the warming during adsorption of VOCs in a fixed bed adsorption. Finally, the breakthrough curves of benzene and MEK were obtained to evaluate the dynamic adsorption performance of two adsorbents.

* Corresponding author. Tel.: +86 25 89680380.
E-mail address: clong@nju.edu.cn (C. Long).

0304-3894/$ – see front matter © 2011 Elsevier B.V. All rights reserved.
doi:10.1016/j.jhazmat.2011.12.010

2. Experimental

2.1. Materials

Styrene, divinylbenzene, benzene, methyl ethyl ketone (MEK) and other reagents were purchased from Shanghai Reagent Station (Shanghai, China) in A.R. grade. The coconut-shell granular activated carbon (m-GAC) was purchased from Liyang Tianlun Environmental Materials Ltd., China.

2.2. Synthesis of a hypercrosslinked adsorbent (HY-1)

The hypercrosslinked polymeric adsorbent was prepared via a post-crosslinking step of low-crosslinked macroporous poly (styrene–divinylbenzene, St–DVB). First, the St–DVB copolymer with cross-linking density of 8% was synthesized by suspension polymerization, in which styrene (92 g) was used as the monomer, divinylbenzene (8 g) as the cross-linked reagent, toluene and n-heptane (50 g) as the mixture porogen, and dibenzoyl peroxide (3 g) as an initiator. The polymerization process was performed at 353 K for 12 h. Then, chloromethylation of the low-crosslinked macroporous copolymer was carried out. 100 g of the obtained low-crosslinked macroporous poly (St–DVB) beads was swollen in 500 mL of monochloromethylether. Then, 40 g of ferric chloride was added slowly. The chloromethylation reaction was done continuously at 311 K for 12 h. Finally, 100 g of choromethylated poly (St–DVB) beads was swollen in 500 mL of 1,2-dichloroethane, which is not only less toxic than nitrobenzene used widely in the synthesis of hypercrosslinked polymer but also can be recovered conveniently and reused. The mixture was further stirred at 353 K for 20 h after 30 g of ferric chloride was added slowly. Finally, the polymer beads filtered and then extracted in a Soxhlet apparatus with ethanol for 8 h and dried under vacuum at 333 K for 8 h.

2.3. Adsorption experiments

The adsorption of benzene and MEK vapors was determined by the column adsorption method. The detailed experimental apparatus and adsorption procedure have been described previously [24]. Briefly, about 1000 g of HY-1 or m-GAC was precisely weighed out and charged into the adsorption column made of glass. The carrier gas containing a scheduled concentration of VOCs vapor was passed through the column until the VOCs concentration become constant and stable, the changes of VOCs concentration in the effluent steam from the adsorption column was measured by using gas chromatography with a quartz capillary column (a length of 30 m, inner diameter of 0.53 mm, and wall thickness of 1.0 μm) and FID detector (SP-6890, Nunan, China) and recorded by a computer. The column temperature was maintained at 60 °C. The detector and injector temperature was maintained at 150 °C and 200 °C, respectively. Nitrogen was used as an inert gas, and hydrogen was used as a fuel gas with air. The equilibrium amount adsorbed was equal to the weight change of adsorbent before and after the adsorption process. Here, a high precision microbalance (BS224S, Sartorius, Germany) was adopted as the weighing device.

3. Results and discussion

3.1. Characterization of adsorbents

The N_2 adsorption–desorption isotherms at 77 K of two adsorbents HY-1, and m-GAC are demonstrated in Fig. 1. It is observed that the initial part of the adsorption isotherms at lower relative pressure (P/P_0) below 0.05, where the nitrogen uptake increases sharply with the increment of relative pressure, proves the existence of micropore structure. According to IUPAC classification,

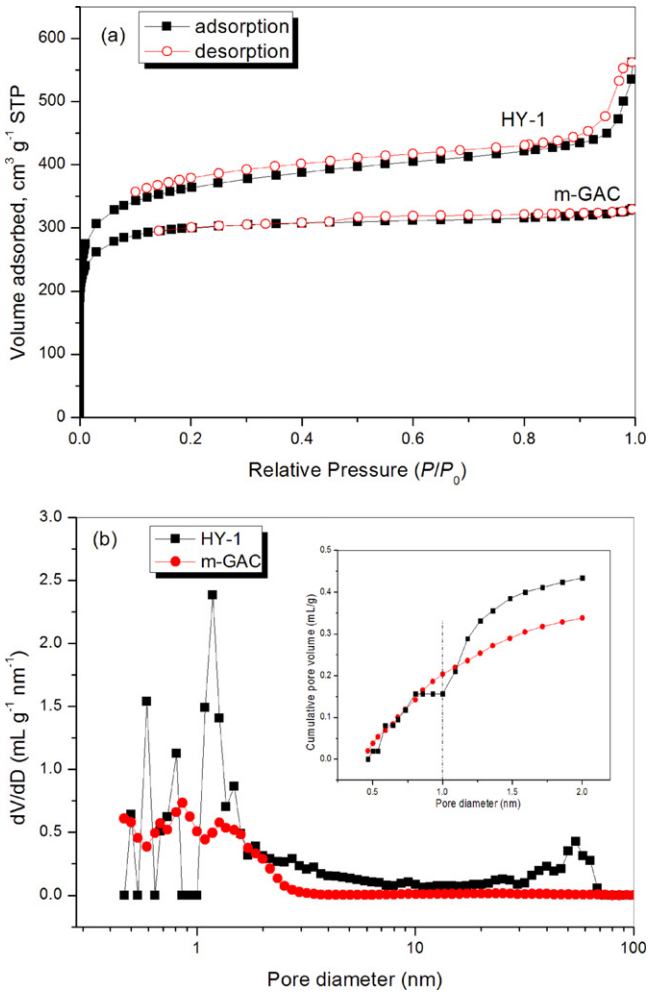

Fig. 1. (a) The N_2 adsorption–desorption isotherms at 77 K, and (b) pore size distribution of HY-1 and m-GAC.

HY-1 and m-GAC are typical of adsorbents with a predominantly microporous structure, as the majority of pore-filling will occur at relative pressures below 0.1. However, for the HY-1, the slope of the plateau at medium relative pressures and accelerated uptakes at higher relative pressure mean that HY-1 also contains a proportion of mesopore and macropore. The pore size distributions of two polymeric adsorbents calculated by applying the density functional theory (DFT) to the N_2 adsorption–desorption isotherms at 77 K are also shown in Fig. 1. It is clearly shown from Fig. 1 that m-GAC is typical of micropore adsorbent with a unimodal pore distribution between 0.5 and 2.0 nm, while HY-1 shows a "bimodal pore system" with both micropore (0.5–2.0 nm) and meso-macropore (30–70 nm). In addition, thermogravimetric analysis (shown in Fig. S1 of Supporting Information) showed that HY-1 exhibits perfect thermostability under 300 °C. Detailed physiochemical properties of two adsorbents used in this study are presented in Table 1.

3.2. Adsorption isotherms

The comparison of the adsorption of benzene and MEK vapor on HY-1 and m-GAC in the range of 303–328 K are provided in Fig. 2. From Fig. 2, it is learned that the adsorption capacities of benzene and MEK on the m-GAC were similar or higher than those of HY-1 at the lower relative pressure studied. Such result may be attributed to the fine microporous structure of m-GAC. From Fig. 1(b), It is clearly shown that m-GAC had a main microporous distribution

Table 1
Salient properties of HY-1 and m-GAC.

Adsorbent	HY-1	m-GAC
Matrix	Hypercroslinked, Styrene–divinylbenzene	Coconut shell based
BET surface area[a] (m^2/g)	1244.2	1015.2
Mesopore volume[a] (mL/g)	0.305	0.081
Micropore volume[a] (mL/g)	0.541	0.407
Average pore diameter (nm)	2.35	1.98
Particle size (mm)	0.4–0.8	0.3–0.6
Contact angle (°C)[b]	127	48
Shape	Spherical	Amorphous

[a] Calculated from the N_2 isotherm data at 77 K by Brunauer–Emmett–Teller (BET), Barrett–Joyner–Halena (BJH), and Dubinin–Astakov (DA) methods, respectively.
[b] Measured by a goniometer (DSA 100, KRUSS, Germany).

between 0.5 and 1.0 nm; Moreover, the micropore volume of m-GAC between 0.5 and 1.0 nm is larger than that of HY-1. Therefore, due to the closer proximity of the walls of micropores, an interaction of the Polanyi potentials may occur resulting in a relatively deep potential energy well and enhanced adsorption of benzene and MEK onto m-GAC than onto HY-1 at a given lower pressure. However, the adsorption capacities of HY-1 for benzene and MEK were larger than those of AC with increasing the relative pressure due to its larger microporous volume. On the other hand, it should be noted that increasing the adsorption temperature from 303 K to 328 K reduced the adsorption capacities of benzene and MEK onto HY-1 more markedly than those onto m-GAC. Such effect of temperature on adsorption capacities of benzene and MEK is more efficient to regenerate HY-1 than m-GAC in a temperature swing adsorption process.

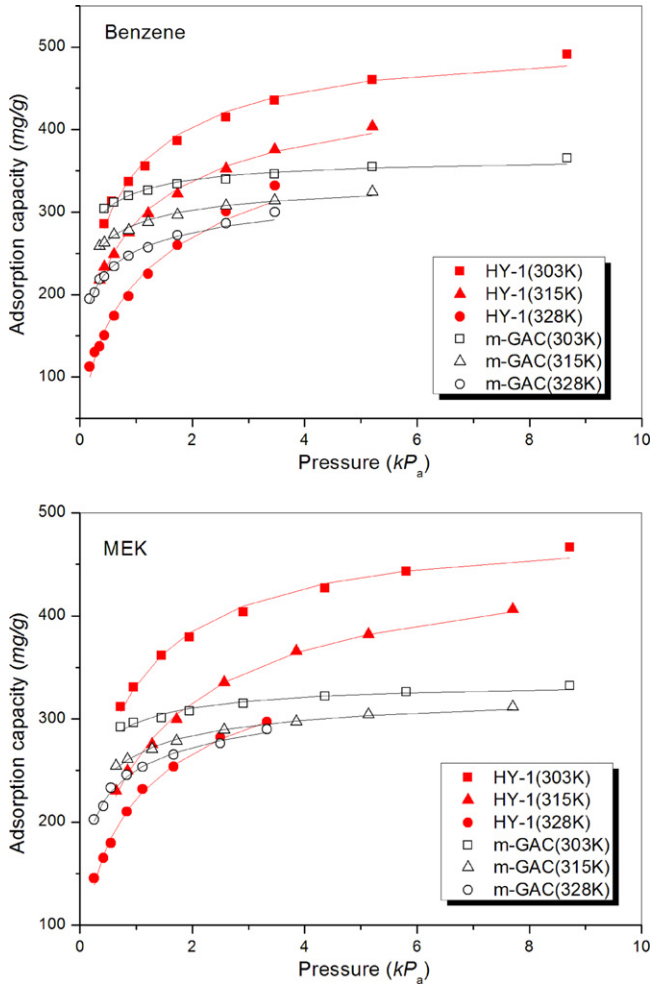

Fig. 2. Equilibrium adsorption data of benzene and MEK onto HY-1 and m-GAC and fitting curves of Dubinin–Radushkevich (D–R) equation as solid lines.

As previously mentioned, HY-1 and m-GAC are primarily microporous adsorbents. Hence, the Dubinin–Radushkevich (D–R) equation, which is widely used for describing the adsorption of organic vapor adsorbates on microporous adsorbents, was chosen to model the adsorption isotherms. The D–R equation can be defined as Eqs. (1)–(3).

$$q_v = q_0 \exp\left[-\left(\frac{\varepsilon}{E}\right)^2\right] \quad (1)$$

$$\varepsilon = RT \ln\left(\frac{P_0}{P}\right) \quad (2)$$

$$q_v = \frac{q}{\rho} \quad (3)$$

where q_v is volume adsorbed capacity (mL/g), q_0 is the limiting microporous volume, ε is the adsorption potential (J/mol) written by Eq. (2), E is the adsorption characteristic energy (kJ mol^{-1}), R is a gas constant, T is the absolute temperature (K), P_0 is the saturation vapor pressure (kPa), P is the equilibrium vapor pressure, q is the equilibrium adsorption amount (mg/g), ρ is the adsorbate density in the adsorbed phase assumed to be the same as that in the liquid phase.

The experimental data of benzene and MEK onto HY-1 and m-GAC at 303 K, 315 K, and 328 K in Fig. 2 are represented as symbols and isotherm fittings using the D–R equation as solid lines. Clearly, the experimental data were well fitted by the D–R equation with all of the regression coefficients (R^2) > 0.96 (Table 2), indicating the suitability of D–R equation for describing the adsorption behavior of the benzene and MEK on HY-1 and m-GAC. The mean values of E and q_0 calculated from three individual values at 303, 315, and 328 K were shown in Table 2. The relative standard deviations for E and q_0 are 1.94–9.24% and 2.01–9.58%, respectively, showing temperature-independent nature of E and q_0, which satisfies the temperature invariance of the Polanyi adsorption potential. This result is important because it allows the use of the D–R equation without introducing any additional parameters to describe the temperature effect on adsorption isotherms for acetone and benzene over the temperature range studied here.

3.3. Isosteric heat of adsorption

The isosteric heats of adsorption (ΔH_{st}) were calculated using Eq. (4) based on the Polanyi adsorption potential and the Clausius–Clapeyron equation according to Ramirez et al. [25]. The derivation of ΔH_{st} and the meaning of physical parameters in Eq. (4) are provided in the Supporting Information.

$$\Delta H_{st} = \frac{RT^2}{P_0}\frac{dP_0}{dT} + E\left(\ln\frac{q_0}{q}\right)^{1/n} + \frac{\alpha TE}{n}\left(\ln\frac{q_0}{q}\right)^{1/n-1} \quad (4)$$

Fig. 3 shows the dependence of isosteric heats ΔH_{st} on adsorbate, temperature, and surface loading. It can be learned from that the effect of temperature on ΔH_{st} was negligible for benzene, and MEK. These results confirm that ΔH_{st} values for both adsorbates are independent of temperature for the conditions studied here. The isosteric enthalpy change accompanying adsorption can be used as a measure of the energetic heterogeneity of a solid surface [26,27]. It is observed that the isosteric enthalpies of adsorption were varied with the surface loading for benzene and MEK, implying that both HY-1 and m-GAC have an energetically heterogeneous surface. The larger change of ΔH_{st} for benzene and MEK on m-GAC with the increase of the adsorbate loading shows more energetic heterogeneity nature than HY-1.

Table 2
The fitting parameters of D–R equation for adsorption of benzene and MEK on HY-1 and m-GAC.

Adsorbent	Adsorbate	Temperature (K)	D–R parameters		
			E (kJ mol^{-1})	q_0 (mL/g)	R^2
HY-1	Benzene	303	12.251	0.553	0.987
		315	13.276	0.500	0.993
		328	12.550	0.483	0.986
			12.692 ± 0.527[a]	0.512 ± 0.071[a]	
	MEK	303	11.964	0.574	0.990
		315	11.939	0.538	0.997
		328	13.971	0.474	0.997
			12.625 ± 1.166[a]	0.529 ± 0.051[a]	
m-GAC	Benzene	303	21.374	0.411	0.969
		315	22.083	0.379	0.985
		328	20.612	0.371	0.992
			21.356 ± 0.736[a]	0.387 ± 0.021[a]	
	MEK	303	20.956	0.410	0.964
		315	20.173	0.394	0.993
		328	20.432	0.400	0.991
			20.520 ± 0.399[a]	0.401 ± 0.008[a]	

[a] The value of E (or n) was calculated as mean ± standard deviation from three individual values at 303, 315, and 328 K

It should be noted in Fig. 3 that m-GAC exhibited much higher values of ΔH_{st} for benzene and MEK than HY-1 at the whole surface loading studied, indicating that m-GAC offered much greater potential in the adsorption and removal of benzene and MEK than HY-1. Such result is consistent with the higher equilibrium adsorption capacities of m-GAC for benzene and MEK than those of HY-1 at lower relative pressure. However, high exothermic heats of adsorption of VOCs onto adsorbent can lead to significant temperature rise during the adsorption step [28], which has a negative impact on the performance of the adsorption unit, such as the reduce of dynamic adsorption capacity and the induction of oxidation reaction.

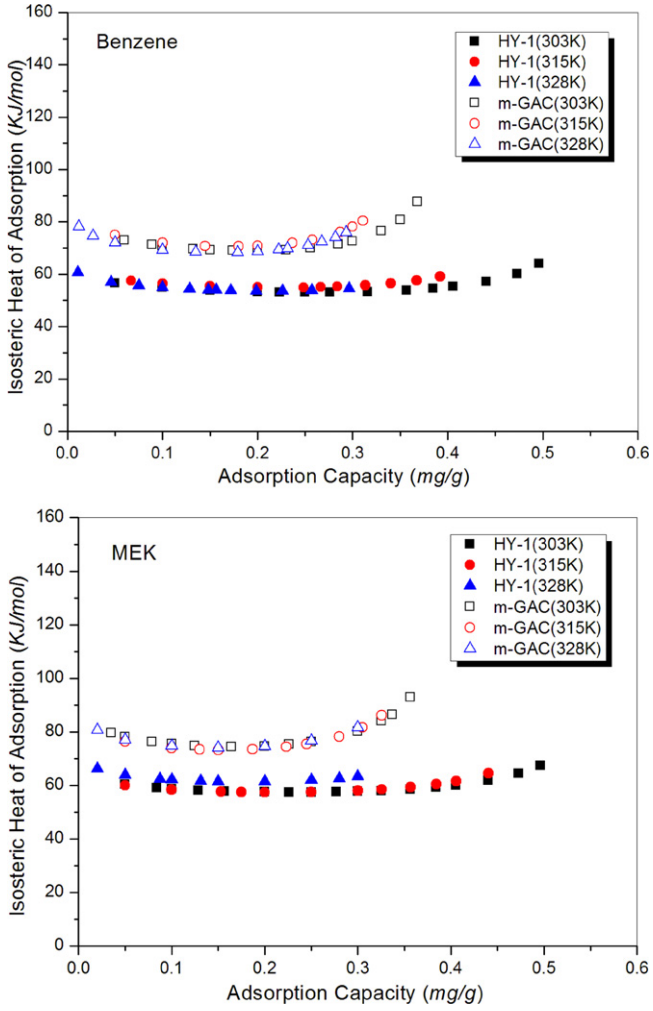

Fig. 3. Isosteric heats of adsorption for the benzene and MEK on HY-1 and m-GAC at different temperatures.

It can be learned from the effect of temperature on ΔH_{st} was negligible for benzene, and MEK. These results confirm that ΔH_{st} values for both adsorbates are independent of temperature for the conditions studied here.

3.4. Breakthrough curves

The actual adsorption processes of VOCs are in many cases associated with adsorption using a fixed bed. A breakthrough curve measurement is a direct method designed to make clear the dynamic performance of VOCs adsorption. The breakthrough curves of benzene and MEK onto HY-1 and m-GAC were shown in Fig. 4. To evaluate quantitatively the dynamic adsorption behavior of benzene and MEK, the breakthrough curves were fitted using the Yoon and Nelson model (Y–N model). The Yoon and Nelson equation is expressed as the following equation [29].

$$t = \tau + \frac{1}{k'} \ln \frac{C_b}{C_i - C_b} \tag{5}$$

where C_i and C_b are inlet and outlet concentration of adsorbate (mg/L), t is the adsorption time (min), k' is the rate constant (min^{-1}), and τ is the time required for 50% adsorbate breakthrough (min).

It was shown clearly from Fig. 4 that the breakthrough curves of benzene and MEK onto HY-1 and GAC were well fitted by the Y–N model. Moreover, HY-1 has an exceptionally good shape of the adsorption breakthrough curves for benzene and MEK, exhibiting a long breakthrough time and a rapid increase after the breakthrough compared with GAC. For the sake of comparison, the calculated breakthrough times and the lengths of mass transfer zone based on the Y–N equation were summarized in Table 3. The breakthrough time is calculated as the time at which the concentration in the outlet is 5% of the inlet concentration. The length of mass transfer zone is calculated by Eq. (6) [30].

$$H_{MTZ} = \frac{2L(T_{0.95} - T_{0.05})}{T_{0.95} - T_{0.05}} \tag{6}$$

where L is the length of the packed bed (cm); $T_{0.05}$ and $T_{0.95}$ are the breakthrough and exhaustion time (min), which are defined as the

Table 3
The breakthrough times and the length of mass transfer zone for benzene and MEK calculated by Y–N equation.

Adsorbent	Adsorbate	Breakthrough time (min)	H_{MTZ} (cm)
HY-1	Benzene	136.1	0.625
	MEK	108.3	1.089
m-GAC	Benzene	121.5	2.328
	MEK	90.98	2.392

times when the outlet concentrations are 5% and 95% of the inlet concentration, respectively.

In general, the longer the breakthrough time is, the higher the dynamic adsorption capacity becomes. Additionally, a more rapid increase in the curve after the breakthrough means less resistance in intraparticle mass transfer. It is learned from Table 3 that the breakthrough times of benzene and MEK onto HY-1 increased by 12.02% and 19.04% than those of m-GAC, respectively. Moreover, the mass transfer zone lengths of benzene and MEK onto HY-1 reduced by 73.15% and 54.47% than those of m-GAC, respectively. A "steeper" mass transfer zone means that more of the bed is used for separation. The good adsorption dynamic VOCs capacity of the HY-1 was attributed to its specific bimodal property in the region of micropore (0.5–2.0 nm) and meso-macropore (30–70 nm). The larger micropore volume of HY-1 directly lead to an increase in the dynamic capacities for benzene and MEK compared to m-GAC. The meso-macropore of HY-1 act as transport pores for benzene and MEK molecules diffusing into the internal surfaces and micropores, and therefore improve the adsorption kinetics.

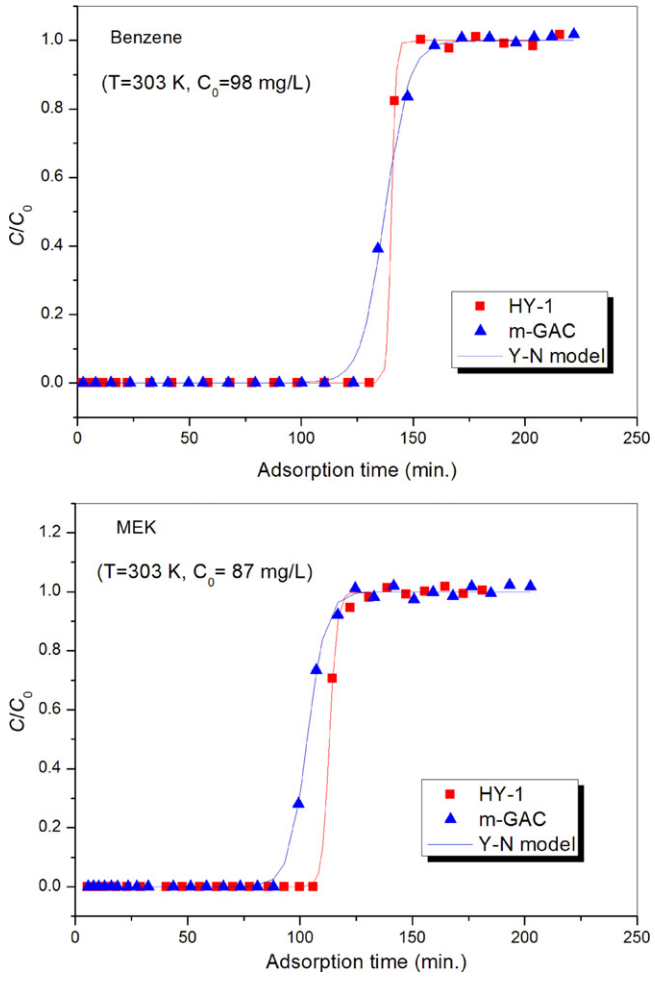

Fig. 4. Experimental breakthrough curves of benzene and MEK adsorption on HY-1 and m-GAC.

4. Conclusions

Adsorption equilibrium of benzene and MEK vapors onto hypercrosslinked polymeric resin and a commercial microporous activated carbon were investigated at 303 K, 315 K, and 328 K, respectively, and favorable adsorption isotherms were exhibited. The experimental data were fitted by the D–R equation with all of the regression coefficients (R^2) > 0.96, indicating the suitability of D–R equation for describing the adsorption behavior of the benzene and MEK on HY-1 and m-GAC. The effect of temperature on the adsorption of benzene and MEK onto HY-1 was more markedly than m-GAC; such effect is more efficient to regenerate the HY-1 in a temperature swing adsorption process.

By calculating the isosteric enthalpies of adsorption, it was found that m-GAC exhibited much wider range and higher values of ΔH_{st} for the VOCs because of its more heterogeneous surface and higher affinity to the VOCs. However, high exothermic heats of adsorption of VOCs onto adsorbent can lead to significant temperature rises during the adsorption step, which can lead to the reduce of dynamic adsorption capacity and the induction of oxidation reaction

In addition, Yoon and Nelson model could predict the whole breakthrough curve of benzene and MEK adsorption on HY-1 and m-GAC. HY-1 had an exceptionally good shape of the adsorption breakthrough curves for benzene and MEK, exhibiting a long breakthrough time and a rapid increase after the breakthrough compared with m-GAC.

Acknowledgments

This research was financially funded by National Natural Science Foundation of China (grant no. 51078180), Natural Science Foundation of Jiangsu Province (grant no. BK2009247), and Resources Key Subject of National High Technology Research & Development Project (863 Project, grant no. 2009AA06Z315). This research was also sponsored by Qing Lan Project of Jiangsu Province, the Fundamental Research Funds for the Central Universities (grant no. 1116021105) and Program for Changjiang Scholars Innovative Research Team in University.

Appendix A. Supplementary data

Supplementary data associated with this article can be found, in the online version, at doi:10.1016/j.jhazmat.2011.12.010.

References

[1] A.K. Ghoshal, S.D. Manjare, Selection of appropriate adsorption technique for recovery of VOCs: an analysis, J. Loss Prevent. Process Ind. 15 (2002) 413–421.
[2] M.J. Ruhl, Recover VOCs via adsorption on activated carbon, Chem. Eng. Prog. 89 (1993) 37–41.
[3] US EPA, Choosing an adsorption system for VOC: carbon, zeolite, or polymers? 5(1999) 456/F-99-004.
[4] G.O. Wood, A review of the effects of covapors on adsorption rate coefficients of organic vapors adsorbed onto activated carbon from flowing gases, Carbon 40 (2002) 685–694.
[5] L. Li, S.Q. Liu, J.X. Liu, Surface modification of coconut shell based activated carbon for the improvement of hydrophobic VOC removal, J. Hazard. Mater. 192 (2011) 683–690.
[6] J.H. Tsai, H.M. Chiang, G.Y. Huang, H.L. Chiang, Adsorption characteristics of acetone, chloroform and acetonitrile on sludge-derived adsorbent, commercial granular activated carbon and activated carbon fibers, J. Hazard. Mater. 154 (2008) 1183–1191.
[7] R.A. Zerbonia, C.M. Brockmann, P.R. Peterson, D. Housley, Carbon bed fires and use of carbon canisters for air emissions control on fixed-roof tanks, J. Air Waste Manage. Assoc. 51 (2001) 1617–1627.

[8] D. Kaplan, I. Nir, L. Shmueli, Effects of high relative humidity on the dynamic adsorption of dimethyl methylphosphonate (DMMP) on activated carbon, Carbon 44 (2006) 3247–3254.
[9] J.K. Brennan, T.J. Bandosz, K.T. Thomson, K.E. Gubbins, Water in porous carbons, Colloid Surf. A: Physicochem. Eng. Aspects 187–188 (2001) 539–568.
[10] Z.Y. Xu, Q.X. Zhang, Herbert H.P. Fang, Applications of porous resin sorbents in industrial wastewater treatment and resource recovery, Crit. Rev. Environ. Sci. Technol. 33 (2003) 363–389.
[11] V.A. Davankov, M.P. Tsyurupa, Structure properties of hypercrosslinked polystyrenes: the first representative of a new class of polymer networks, React. Polym. 13 (1990) 27–42.
[12] M.P. Tsyurupa, V.A. Davankov, Porous structure of hypercrosslinked polystyrene: state-of-the-art mini-review, React. Funct. Polym. 66 (2006) 768–779.
[13] N. Fontanals, M. Galià, P.A.G. Cormack, R.M. Marcé, D.C. Sherrington, F. Borrull, Evaluation of a new hypercrosslinked polymer as a sorbent for solid-phase extraction of polar compounds, J. Chromatogr. A 1075 (2005) 51–56.
[14] C. Valderrama, X. Gamisans, F.X. de las Heras, J.L. Cortina, A. Farran, Kinetics of polycyclic aromatic hydrocarbons removal using hyper-cross-linked polymeric sorbents Macronet Hypersol MN200, React. Funct. Polym. 67 (2007) 1515–1529.
[15] L. Chao, A.M. Li, H.S. Wu, Q.X. Zhang, Adsorption of naphthalene onto macroporous and hypercrosslinked polymeric adsorbent: effect of pore structure of adsorbents on thermodynamic and kinetic properties, Colloids Surf. A 333 (2009) 150–155.
[16] J. Huang, K. Huang, C. Yan, Application of an easily water-compatible hypercrosslinked polymeric adsorbent for efficient removal of catechol and resorcinol in aqueous solution, J. Hazard. Mater. 167 (2009) 69–74.
[17] J. Huang, Treatment of phenol and p-cresol in aqueous solution by adsorption using a carbonylated hypercrosslinked polymeric adsorbent, J. Hazard. Mater. 168 (2009) 1028–1034.
[18] V.V. Podlesnyuk, J. Hradil, E. Králová, Sorption of organic vapours by macroporous and hypercrosslinked polymeric adsorbents, React. Funct. Polym. 42 (1999) 181–191.
[19] E.J. Simpson, W.J. Koros, R.S. Schechter, An emerging class of volatile organic compound sorbents: Friedel-Crafts modified polystyrenes. 1. Synthesis, characterization, and performance in aqueous- and vapor-phase applications, Ind. Eng. Chem. Res. 35 (1996) 1195–1205.
[20] E.J. Simpson, W.J. Koros, R.S. Schechter, An emerging class of volatile organic compound sorbents: Friedel-Crafts modified polystyrenes. 2. Performance comparison with commercially-available sorbents and isotherm analysis, Ind. Eng. Chem. Res. 35 (1996) 4635–4645.
[21] M.P. Baya, P.A. Panayotis, V.A. Davankov, Evaluation of a hypercrosslinked polystyrene, MN-200, as a sorbent for the preconcentration of volatile organic compounds in air, J. Assoc. Off. Anal. Chem. Int. 83 (2000) 579–583.
[22] P. Liu, C. Long, Q.F. Li, H.M. Qian, A.M. Li, Q.X. Zhang, Adsorption of trichloroethylene and benzene vapors onto hypercrosslinked polymeric resin, J. Hazard. Mater. 166 (2009) 6–51.
[23] C. Long, Q.F. Li, Y. Li, Y. Liu, A.M. Li, Q.X. Zhang, Adsorption characteristics of benzene-chlorobenzene vapor on hypercrosslinked polystyrene adsorbent and a pilot-scale application study, Chem. Eng. J. 160 (2010) 723–728.
[24] C. Long, P. Liu, Y. Li, A.M. Li, Q.X. Zhang, Characterization of hydrophobic hypercrosslinked polymer as an adsorbent for removal of chlorinated volatile organic compounds, Environ. Sci. Technol. 45 (2011) 4506–4512.
[25] D. Ramirez, S.Y. Qi, M.J. Rood, Equilibrium and heat of adsorption for organic vapors and activated carbons, Environ. Sci. Technol. 39 (2005) 5864–5871.
[26] D.D. Do, H.D. Do, A new adsorption isotherm for heterogeneous adsorbent based on the isosteric heat as a function of loading, Chem. Eng. Sci. 52 (1997) 297–310.
[27] F. Delage, P. Pré, P.L. Cloirec, Mass transfer and warming during adsorption of high concentrations of VOCs on an activated carbon bed: experimental and theoretical analysis, Environ. Sci. Technol. 34 (2000) 4816–4821.
[28] S. Giraudet, P.L. Pré, P. Cloirec, Modeling the heat and mass transfers in temperature-swing adsorption of volatile organic compounds onto activated carbons, Environ. Sci. Technol. 43 (2009) 1173–1179.
[29] Y.H. Yoon, J.H. Nelson, Application of gas adsorption kinetics I: A theoretical model for respirator cartridge service life, Am. Ind. Hyg. Assoc. J. 45 (1984) 509–516.
[30] A.A. Pota, A.P. Mathews, Effects of particle stratification on fixed bed adsorber performance, J. Environ. Eng. 125 (1999) 705–711.